Supporting information

Remarkable Elasticity and Enzymatic Degradation of Bio-based Poly(butylene adipate-co-furanoate): Replacing terephthalate

*Hyeri Kim,[a]‡ Taeho Kim,‡[a] Sejin Choi,[a] Hyeonyeol Jeon,[a] Dongyeop X. Oh,[a.b] Jeyoung Park,[a,b] Youngho Eom,[*c] Sung Yeon Hwang,[*a,b] and Jun Mo Koo[*a]*

[a]*Research Center for Bio-based Chemistry, Korea Research Institute of Chemical Technology (KRICT), Ulsan 44429, Republic of Korea. E-mail: crew75@krict.re.kr, jmkoo@krict.re.kr*

[b]*Advanced Materials and Chemical Engineering, University of Science and Technology (UST), Daejeon 34113, Republic of Korea*

[c]*Department of Polymer Engineering, Pukyong National University, Busan, 48513, Republic of Korea. E-mail: eomyh@pknu.ac.kr*

†Electronic supplementary information (ESI) available: Experimental section and complete characterization data. See DOI:

‡These authors contributed equally.

Tel.: +82-52-241-6313 Fax.: +82-52-241-6349 E-mail: eomyh@pknu.ac.kr ORCID: 0000-0002-0922-1155

Tel.: +82-52-241-6321 Fax.: +82-52-241-6349 E-mail: jmkoo@krict.re.kr ORCID: 0000-0002-4485-2155

Tel.: +82-52-241-6313 Fax.: +82-52-241-6349 E-mail: crew75@krict.re.kr ORCID: 0000-0002-4618-2132

Table S1. Characteristic properties of PBAFs and PBATs polymerized with different feed ratio

Sample code	Feed ratio (Aro. : Ali. : BD)*	BF or BT (mol%)	M_n (g mol^{-1})	M_w (g mol^{-1})	PDI
PBAF50	5 : 5 :16	49.2	44,000	87,000	1.98
PBAF60	6 : 4 :16	58.5	45,600	90,400	1.98
PBAF70	7 : 3 :16	68.9	47,300	95,000	2.01
PBAF80	8 : 2 :16	78.9	47,400	85,800	1.81
PBAT50	5 : 5 :16	51.9	45,100	93,000	2.06
PBAT60	6 : 4 :16	62.7	44,000	87,000	198
PBAT70	7 : 3 :16	72.2	49,300	104,600	2.12
PBAT80	8 : 2 :16	81.3			

* : Aro. is DMFD or DMT as aromatic acidic monomer, and Ali. is AA as aliphatic acidic monomer

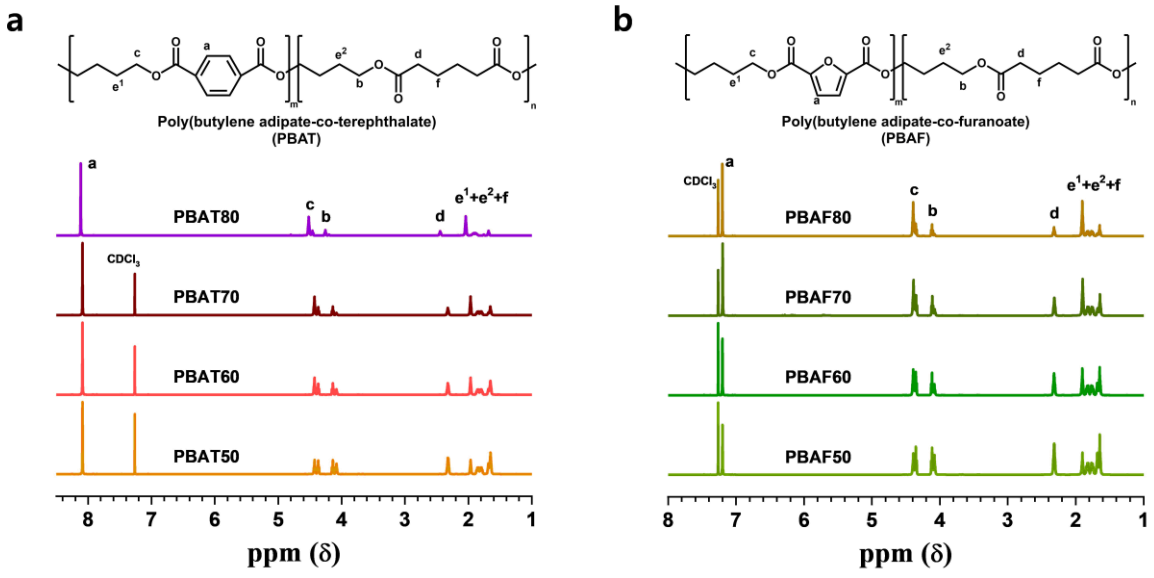

Fig. S1. ^{1}H NMR spectra of (a) PBATs and (b) PBAFs copolyesters with different aromatic content.

Table S2. Sequence distribution of PBAT and PBAF copolyesters.

Sample code	Dyad fraction[a]				Probability factor		Block length[b]		R[c]
	$f_{Ar/Ar}$[b]	$f_{Ar/Al}$	$f_{Al/Ar}$	$f_{Al/Al}$	$P_{Ar/Al}$	$P_{Al/Ar}$	L_{Ar}	L_{Al}	
PBAF50	0.253	0.258	0.257	0.232	0.524	0.506	1.907	1.977	1.030
PBAF60	0.355	0.252	0.241	0.153	0.431	0.580	2.322	1.725	1.010
PBAF70	0.475	0.231	0.205	0.089	0.335	0.659	2.984	1.517	0.994
PBAF80	0.620	0.183	0.157	0.040	0.232	0.745	4.302	1.342	0.978
PBAT50	0.269	0.260	0.249	0.223	0.528	0.490	1.893	2.041	1.018
PBAT60	0.392	0.239	0.232	0.137	0.409	0.560	2.447	1.785	0.969
PBAT70	0.521	0.206	0.197	0.077	0.299	0.633	3.343	1.580	0.932
PBAT80	0.639	0.159	0.171	0.031	0.202	0.811	4.954	1.233	1.013

[a] Molar fraction of dyad containing Ar (aromatic segment) or Al (aliphatic segment) on each side of BD.

Dyad fraction was estimated experimentally by deconvoluting the ^{1}H NMR spectra shown in **Fig. S2**

[b] Block length was calculated using the **Equation 1** and from Ref. 50

[c] Degree of randomness

Equation 1.

$$P_{Ar/Al} = \frac{f_{Ar/Al}}{f_{Ar}}$$

$$P_{Al/AR} = \frac{f_{Al/Ar}}{f_{Al}}$$

$$L_{Ar} = \frac{1}{P_{Ar/Al}}$$

$$L_{Al} = \frac{1}{P_{Al/Ar}}$$

$$R = P_{Ar/Al} + P_{Al/Ar}$$

Here, L_{Ar} and L_{Al} represent the number-average sequence length of the aromatic (TPA/FDCA) and aliphatic segments (AA), respectively.

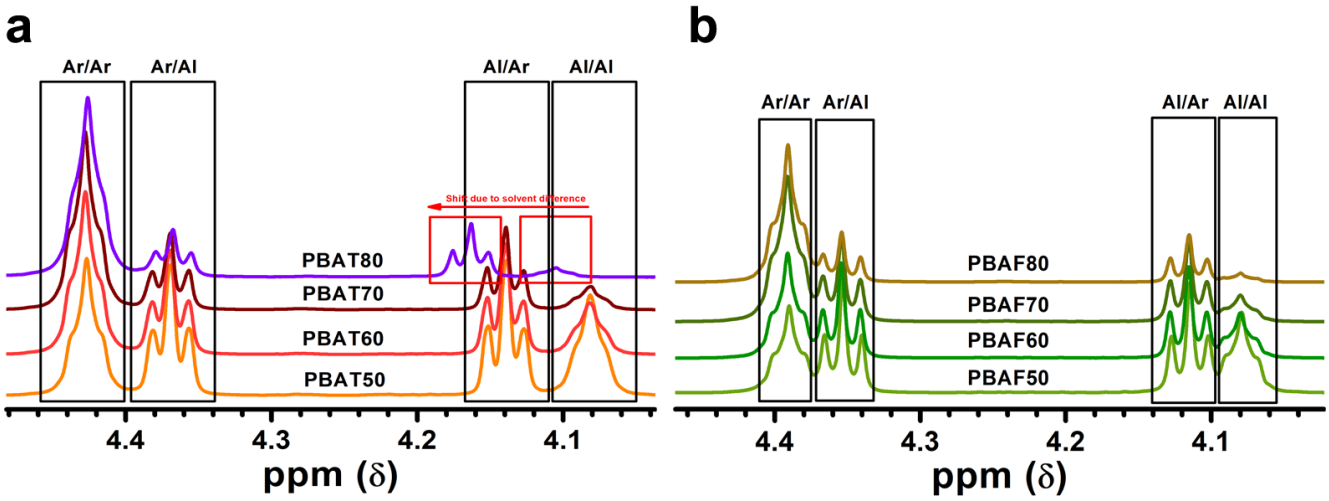

Fig. S2. Magnified ^{1}H NMR for sequence distribution calculation.

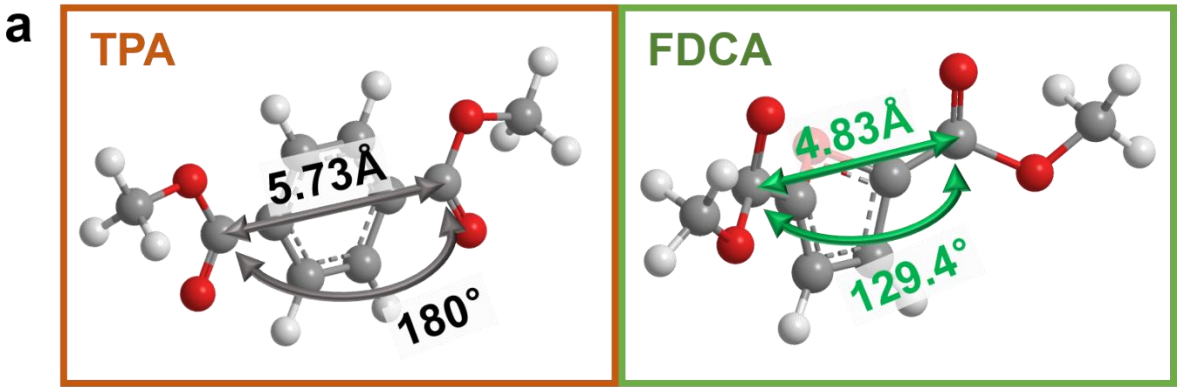

Fig. S3. Molecular structure of planar TPA and distorted FDCA.

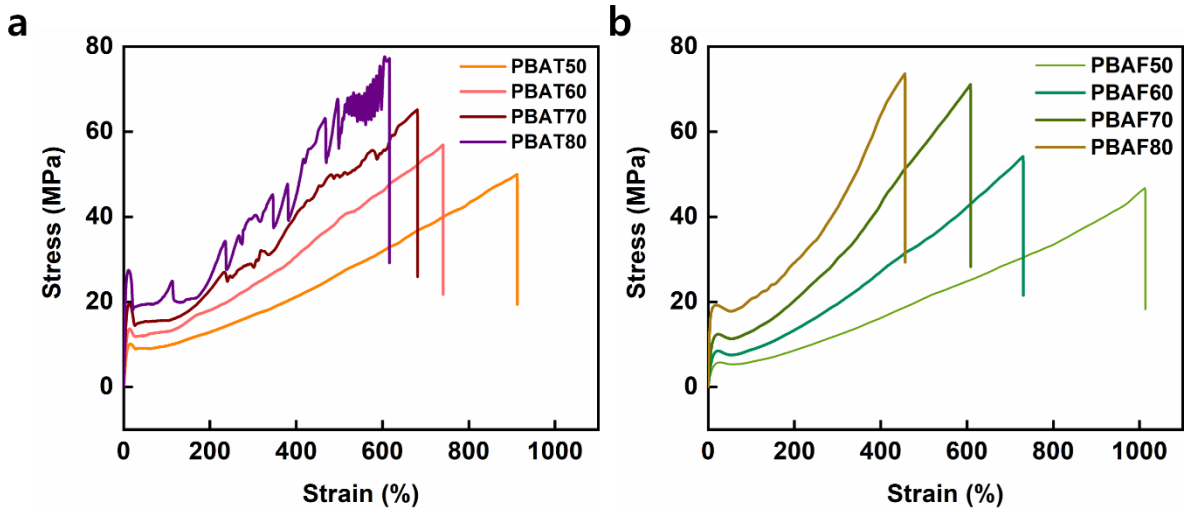

Fig. S4. Stress-Strain curves of (a) PBATs and (b) PBAFs with different aromatic content.

Table S3. Mechanical properties of PBAFs and PBATs with different composition ratio

Code	Young's modulus (MPa)	Tensile Strength (MPa)	Elongation at break (%)
PBAF50	58.4 (0.3)	49.2 (3.4)	1035 (31)
PBAF60	100.8 (3.3)	55.4 (5.9)	733 (58)
PBAF70	167.2 (8.5)	72.8 (3.0)	617 (22)
PBAF80	550.9 (36.9)	74.7 (8.5)	467 (57)
PBAT50	91.1 (11.1)	49.7 (0.4)	876 (50)
PBAT60	153.3 (8.7)	57.1 (0.3)	745 (9)
PBAT70	341.2 (84.5)	70.0 (6.9)	722 (57)
PBAT80	798.0 (22.6)	78.2 (0.9)	606 (2)

The value in parentheses is standard deviation.

Movie S1. Elastic recovery comparison between PBAT50 and PBAF50

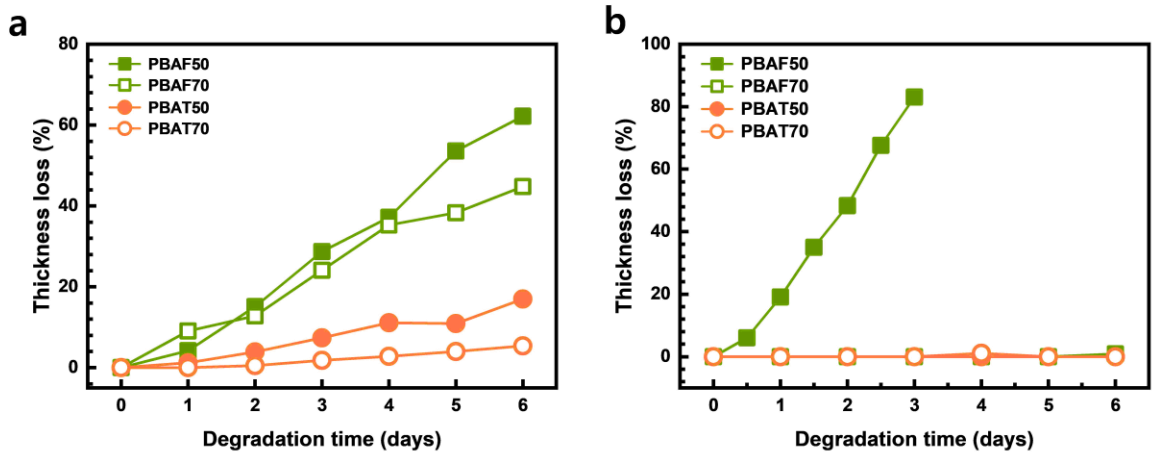

Fig. S5. (a) Chemical and (b) enzymatic degradation analysis on PBAT/F 50 and 70 showing thickness reduction.

Table S4. Thermal properties of PBAFs and PBATs analyzed by DSC

Code	1st heating scan				Cooling scan	2nd heating scan			
	T_{m1} (℃)	ΔH_{m1} (J/g)	T_{m2} (℃)	ΔH_{m2} (J/g)	T_{mc} (℃)	T_g (℃)	T_{cc} (℃)	T_{m2} (℃)	ΔH_{m2} (J/g)
PBAF50	53.6	8.7	93.0	2.2	-	-19.0	-	-	-
PBAF60	56.4	8.7	111.1	9.1	-	-7.0	-	-	-
PBAF70	56.6	6.8	126.1	14.1	-	3.9	94.5	127.5	6.0
PBAF80	58.2	6.1	139.6	20.3	-	14.1	94.5	139.2	9.1
PBAT50	56.1	3.8	137.1	18.2	78.7	ND*	-	138.1	7.5
PBAT60	54.3	1.2	160.1	15.4	133.3	ND*	-	163.0	4.3
PBAT70	55.6	1	176.8	18.1	155.2	ND*	-	179.1	9.7
PBAT80	57.9	1.1	193.0	25.0	176.9	ND*	-	193.3	11.9

*ND : Not detected (in DSC analysis)

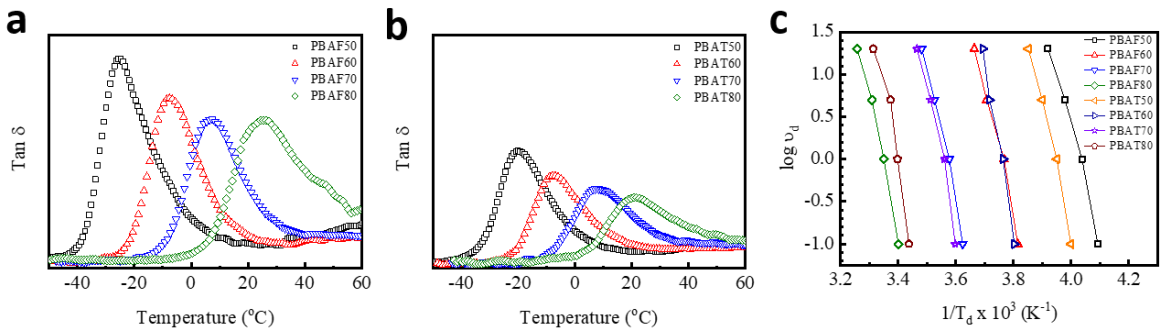

Fig. S6. Tan δ plot obtained DMA analysis at a frequency of 1 Hz of (a) PBAF and (b) PBAT. (c) Arrhenius plot as determined from the changes of peak in tan δ plot with different frequency.

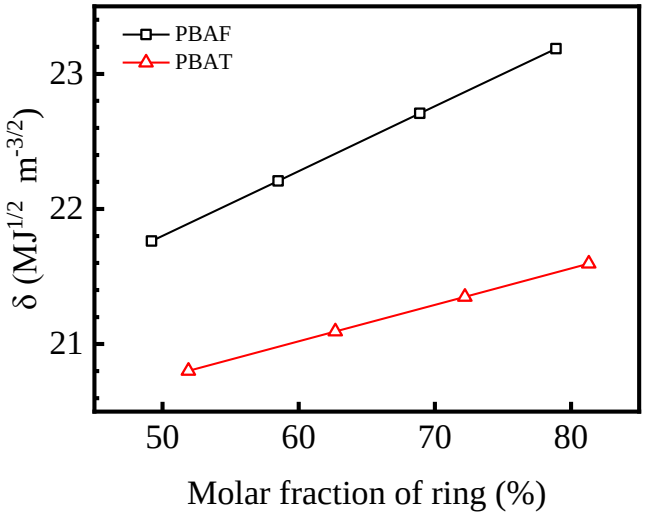

Fig. S7. Solubility parameters of PBATs and PBAFs using Van Krevelen group contribution method.

Table. S5. Individual and total solubility parameters of PBATs and PBATs using Van Krevelen group contribution method

	δ	δ_d	δ_p	δ_h	V_m
PBF	24.2	20.4	6.1	11.4	131.8
PBA	19.4	17.8	4.2	6.5	164.8
PBT	22.1	20.5	4.6	6.8	152.8
PBAF50	21.8	19.1	5.1	8.9	148.6
PBAF60	22.2	19.3	5.3	9.4	145.5
PBAF70	22.7	19.6	5.5	9.9	142.1
PBAF80	23.2	19.9	5.7	10.4	138.8
PBAT50	20.8	19.2	4.4	6.7	158.6
PBAT60	21.1	19.5	4.5	6.7	157.3
PBAT70	21.3	19.7	4.5	6.7	156.1
PBAT80	21.6	20.0	4.5	6.7	155.0

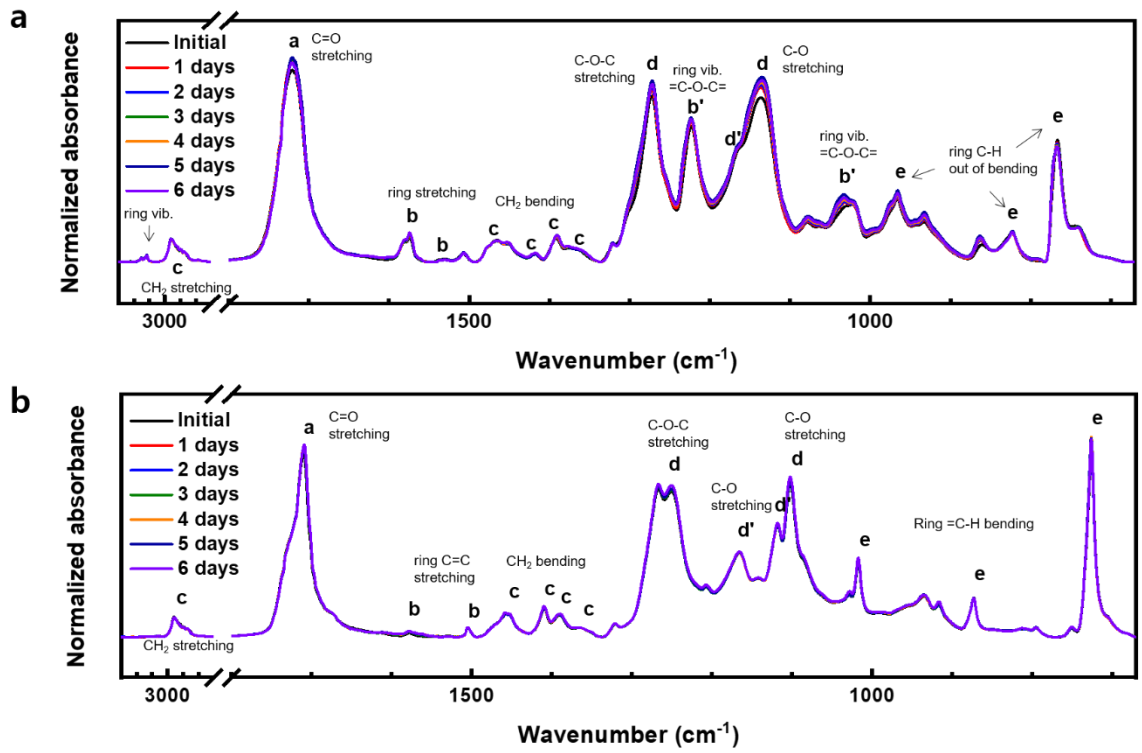

Fig. S8. One dimensional FT-IR spectra of (a) PBAF50, (b) PBAT50 during chemical degradation.

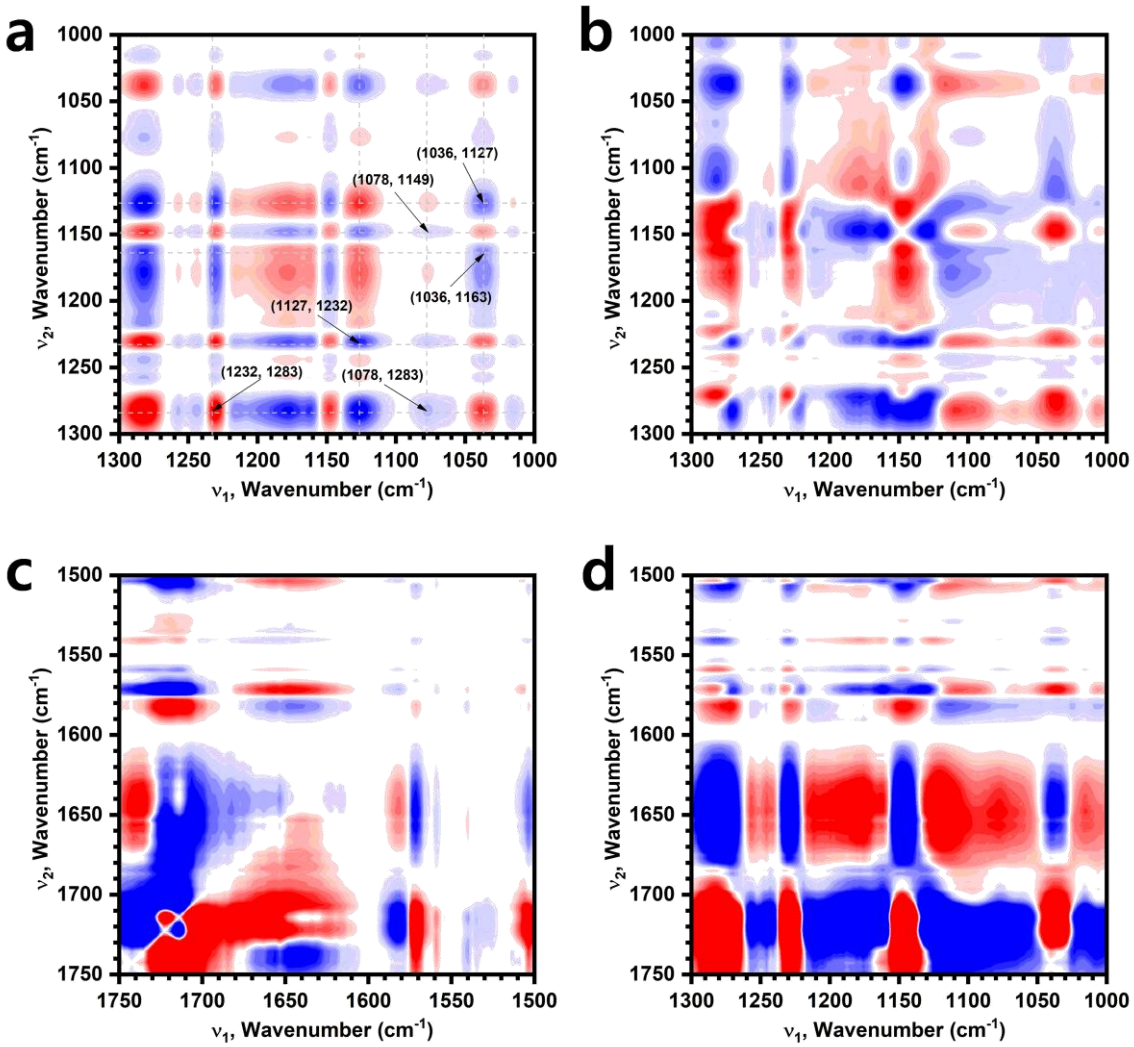

Fig. S9. (a) Synchronous homogeneous 2DCOS in range of 1300-1000 cm^{-1}. (b) and (c) Asynchronous homogeneous 2DCOS in range of 1300-1000 and 1750-1500 cm^{-1}, respectively. (d) Asynchronous heterogeneous 2DCOS (X: 1300-1000, Y: 1750-1500 cm^{-1})

Table S6. 2DCOS analysis of PBAF50 during enzymatic degradation and corresponding sequences and intensity changes.

Sequential order	Wavenumber (cm^{-1})	Intensity change	Assignment
1	1717	▼	C=O adjacent to furan ring
2	1731	▼	C=O from aliphatic segment
3	1654	▲	C=O from FDCA
4	1583	▼	Furan ring stretching
5	1507	▲	Furan ring stretching
6	1163	▼	C-O stretching
7	1036	▲	=C-O-C= ring vibration
8	1127	▼	C-O stretching
9	1232	▲	=C-O-C= ring vibration
10	1283	▲	C-O stretching
11	1574	▲	Furan ring stretching
12	1149	▲	C-O stretching